

Optimal Receiver Placement for Collaborative Mapping of Signals of Opportunity

Joshua J. Morales and Zaher M. Kassas
University of California, Riverside

BIOGRAPHIES

Joshua J. Morales is pursuing a Ph.D. from the Department of Electrical and Computer Engineering at The University of California, Riverside. He received a B.S. in Electrical Engineering with High Honors from The University of California, Riverside. His research interests include estimation, navigation, computer vision, autonomous vehicles, and intelligent transportation systems.

Zaher (Zak) M. Kassas is an assistant professor at The University of California, Riverside. He received a B.E. in Electrical Engineering from The Lebanese American University, an M.S. in Electrical and Computer Engineering from The Ohio State University, and an M.S.E. in Aerospace Engineering and a Ph.D. in Electrical and Computer Engineering from The University of Texas at Austin. From 2004 through 2010 he was a research and development engineer with the LabVIEW Control Design and Dynamical Systems Simulation Group at National Instruments Corp. His research interests include estimation, navigation, autonomous vehicles, and intelligent transportation systems.

ABSTRACT

Mapping an unknown terrestrial signal of opportunity (SOP) via multiple collaborating receivers is considered. The receivers are assumed to have knowledge about their own states, make pseudorange observations on an unknown SOP, and fuse these pseudoranges through a central estimator. Two problems are considered. The first problem assumes N receivers with random initial states to pre-exist in the environment. The question of where to optimally place an additional receiver so to maximize the estimate quality of the SOP's states is addressed. Three optimization problems are compared: minimizing the geometric dilution of precision (GDOP), maximizing the determinant of the GDOP matrix, and maximizing the area of the polygon inscribed in the unit circle whose vertices are the unit line of sight vectors from the SOP to the receivers. It is demonstrated that the three optimization problems are comparable and it is shown that the area maximization problem is piecewise-concave with a simple analytical solution. The second problem addresses the optimal estimation performance as a function of time and number of receivers in the environment. It is demonstrated that such optimal performance assessment could be generated offline without knowledge of the receivers' initial states and trajectories or the receivers' estimates of the SOP.

I. INTRODUCTION

Opportunistic navigation (OpNav) aims to exploit ambient radio signals of opportunity (SOPs) in the environment to enable navigation whenever global navigation satellite system (GNSS) signals become inaccessible or untrustworthy [1, 2]. SOPs include AM/FM radio [3], cellular [4], television [5], Iridium [6], and Wi-Fi [7].

In contrast to GNSS signals, SOPs are not intended for navigation. In particular, while information about GNSS satellite vehicle (SV) states are readily accessible, the states of SOPs may not be known *a priori*. Therefore, a first step in exploiting SOPs is to estimate their states. This can be accomplished either (i) in a mapping framework in which the receivers have knowledge of their own states (by having access to GNSS signals, for example) [8, 9] or (ii) in a simultaneous localization and mapping framework in which the receivers' states are simultaneously estimated with the SOPs' states [10–12].

Collaboration generally improves navigation [13, 14]. In collaborative opportunistic navigation (COpNav), multiple receivers share their observations of SOPs in the environment to construct and continuously refine a global signal landscape map. Such signal landscape could be cloud-hosted, such that whenever GNSS signals become inaccessible or untrustworthy, the receivers continue navigating with the aid of this map [15, 16]. The quality of the constructed map depends on the quality of the observations and the spatial geometry between the SOPs and receivers. In [17–20], the quality of the constructed map was addressed by optimizing the receivers' trajectories, while assuming the initial location of all receivers to be random.

This paper considers the following two problems. The first problem assumes that multiple receivers with random initial states are dropped in a planar COpNav environment with one unknown SOP. Each receiver has *a priori* knowledge about its own states (e.g., from GNSS observables). The receivers draw pseudorange observations from the SOP, which are fused through a centralized estimator that estimates the states of the SOP. Where should an additional collaborating receiver be placed to minimize the uncertainty about the SOP's states? The second problem considers a planar environment comprising N mobile receivers with knowledge about their own states, making pseudorange observations on one unknown terrestrial SOP, and fusing their observations through a centralized esti-

mator. What is the optimal estimation performance as a function of time and N ?

Similar questions to the first problem this paper considers have arisen in other contexts, such as optimal GNSS SV distribution and selection [21–24] and optimal sensor placement for target localization and tracking [25–28]. Common metrics to assess the quality of the spatial geometry are the geometric dilution of precision (GDOP) [29], the determinant of the GDOP matrix [21], and the area of a polygon inscribed in the unit circle whose vertices are the line of sight (LOS) vectors from the receiver (target) to the SVs (sensors) [30]. While previous work considered optimizing the location of a constellation of SVs or a group of sensors with respect to a specified criterion, this paper assumes that N of the receivers are arbitrarily placed, and treats the problem of optimal placement of an additional $(N + 1)^{\text{st}}$ receiver to improve the estimate of the SOP's states. To this end, the GDOP minimization, determinant of GDOP matrix maximization, and area maximization problems are compared and it is demonstrated that these three optimization problems are comparable. Then, it is shown that the area maximization problem is piecewise-concave with a simple analytical solution.

The remainder of this paper is organized as follows. Section II describes the SOP dynamics and receivers' observation model. Section III formulates the optimal receiver placement problem as GDOP minimization, determinant of GDOP matrix maximization, and area maximization and compares these optimization problems. The piecewise-concavity of the area maximization problem is also shown and the optimal solution is specified. Section IV derives the optimal estimation performance as a function of time and number of receivers. Concluding remarks are given in Section V.

II. MODEL DESCRIPTION

A. SOP Dynamics Model

The SOP will be assumed to emanate from a spatially-stationary terrestrial transmitter, and its state vector will consist of its planar position states $\mathbf{r}_s \triangleq [x_s, y_s]^T$ and clock error states $c \mathbf{x}_{\text{clk},s} \triangleq c [\delta t_s, \dot{\delta t}_s]^T$, where c is the speed of light, δt_s is the clock bias, and $\dot{\delta t}_s$ is the clock drift [12]. The SOP's discrete-time (DT) model sampled at a constant sampling interval T is given by

$$\mathbf{x}_s(k+1) = \mathbf{F}_s \mathbf{x}_s(k) + \mathbf{w}_s(k), \quad k = 1, 2, \dots,$$

where $\mathbf{x}_s = [\mathbf{r}_s^T, c \mathbf{x}_{\text{clk},s}^T]^T$, \mathbf{w}_s is a DT zero-mean white noise sequence with covariance \mathbf{Q}_s , and

$$\mathbf{F}_s = \text{diag} [\mathbf{I}_{2 \times 2}, \mathbf{F}_{\text{clk}}], \quad \mathbf{F}_{\text{clk}} = \begin{bmatrix} 1 & T \\ 0 & 1 \end{bmatrix}.$$

B. Observation Model

The pseudorange observation made by the i^{th} receiver on the SOP, after discretization and mild approximations discussed in [12], is related to the SOP states by

$$z_i(k) = \|\mathbf{r}_{r_i}(k) - \mathbf{r}_s\|_2 + c \cdot [\delta t_{r_i}(k) - \delta t_s(k)] + v_i(k), \quad (1)$$

where $\mathbf{r}_{r_i} \triangleq [x_{r_i}, y_{r_i}]^T$ and δt_{r_i} are the position and clock bias of the receiver, respectively, and v_i is a DT zero-mean white Gaussian sequence with variance σ_i^2 .

III. OPTIMAL RECEIVER PLACEMENT

This section tackles the question of: where to optimally place a receiver in a COpNav environment comprising N pre-deployed receivers and one unknown SOP? The following subsection will formulate and compare three optimization problems: GDOP minimization, determinant maximization, and area maximization. Subsequently, the convexity of these problems is analyzed. Finally, an analytical solution to the area maximization problems is derived.

A. Problem Formulation

Consider a planar environment comprising N arbitrarily placed receivers with knowledge about their own states and one unknown SOP. The receivers draw pseudorange observations $\{z_i\}_{i=1}^N$ from the SOP, and these observations are fused through a centralized estimator whose role is to estimate the state vector of the SOP. It is desired to deploy an additional receiver to a location that will result in the maximum improvement of the SOP's state vector estimate. The measurement residual computed by the centralized estimator has a first-order approximation of its Taylor series expansion about an estimate of the SOP's state vector $\hat{\mathbf{x}}_s$ given by

$$\Delta \mathbf{z} = \mathbf{H} \Delta \mathbf{x}_s + \mathbf{v},$$

where $\Delta \mathbf{z} \triangleq \mathbf{z} - \hat{\mathbf{z}}$, i.e., the difference between the observation vector $\mathbf{z} \triangleq [z_1, \dots, z_{N+1}]^T$ and its estimate $\hat{\mathbf{z}}$; $\Delta \mathbf{x} \triangleq \mathbf{x}_s - \hat{\mathbf{x}}_s$, i.e., the difference between the SOP's state vector \mathbf{x}_s and its estimate $\hat{\mathbf{x}}_s$; $\mathbf{v} \triangleq [v_1, \dots, v_{N+1}]^T$; and \mathbf{H} is the Jacobian matrix evaluated at the estimate $\hat{\mathbf{x}}_s$, which is given by

$$\mathbf{H} = \begin{bmatrix} -\frac{x_{r_1} - \hat{x}_s}{\|\mathbf{r}_{r_1} - \hat{\mathbf{r}}_s\|} & -\frac{y_{r_1} - \hat{y}_s}{\|\mathbf{r}_{r_1} - \hat{\mathbf{r}}_s\|} & -1 & 0 \\ -\frac{x_{r_2} - \hat{x}_s}{\|\mathbf{r}_{r_2} - \hat{\mathbf{r}}_s\|} & -\frac{y_{r_2} - \hat{y}_s}{\|\mathbf{r}_{r_2} - \hat{\mathbf{r}}_s\|} & -1 & 0 \\ \vdots & \vdots & \vdots & \vdots \\ -\frac{x_{r_{N+1}} - \hat{x}_s}{\|\mathbf{r}_{r_{N+1}} - \hat{\mathbf{r}}_s\|} & -\frac{y_{r_{N+1}} - \hat{y}_s}{\|\mathbf{r}_{r_{N+1}} - \hat{\mathbf{r}}_s\|} & -1 & 0 \end{bmatrix}. \quad (2)$$

Assuming the observation noise $\{v_i\}_{i=1}^{N+1}$ to be independent and identically distributed, i.e., $\text{cov}(\mathbf{v}) = \sigma^2 \mathbf{I}$, and the centralized estimator to be a static, weighted least-squares estimator, it is obvious that all SOP's states are

observable, except for the SOP's clock drift δt_s , for all $N \geq 2$, and as long as there exists at least three receivers that are not collinear with the LOS vectors connecting the SOP and the receivers [12]. Define the truncated SOP state vector as $\mathbf{x}'_s \triangleq [x_s, y_s, c\delta t_s]^\top$ and adjust the estimator to estimate \mathbf{x}'_s accordingly. Then, \mathbf{H} reduces to

$$\mathbf{H} = \begin{bmatrix} -\hat{\mathbf{1}}_1^\top & -1 \\ -\hat{\mathbf{1}}_2^\top & -1 \\ \vdots & \vdots \\ -\hat{\mathbf{1}}_{N+1}^\top & -1 \end{bmatrix} = \begin{bmatrix} -\cos(\phi_1) & -\sin(\phi_1) & -1 \\ -\cos(\phi_2) & -\sin(\phi_2) & -1 \\ \vdots & \vdots & \vdots \\ -\cos(\phi_{N+1}) & -\sin(\phi_{N+1}) & -1 \end{bmatrix},$$

where $\hat{\mathbf{1}}_i \triangleq \frac{\mathbf{r}_{r_i} - \hat{\mathbf{r}}_s}{\|\mathbf{r}_{r_i} - \hat{\mathbf{r}}_s\|}$, which is geometrically a unit LOS vector pointing from the SOP's position estimate $\hat{\mathbf{r}}_s$ to the i th receiver position \mathbf{r}_{r_i} . Without loss of generality, assume a coordinate frame centered at $\hat{\mathbf{r}}_s$ and ϕ_i to be the angle measured counterclockwise from the LOS vector connecting the SOP and the first receiver (i.e., $\phi_1 = 0$). The weighted least-squares estimate $\hat{\mathbf{x}}'_s$ and associated estimation error covariance $\mathbf{P}_{\hat{\mathbf{x}}'_s \hat{\mathbf{x}}'_s}$ are given by

$$\hat{\mathbf{x}}'_s = (\mathbf{H}^\top \mathbf{H})^{-1} \mathbf{H}^\top \mathbf{z}, \quad \mathbf{P}_{\hat{\mathbf{x}}'_s \hat{\mathbf{x}}'_s} = \sigma^2 (\mathbf{H}^\top \mathbf{H})^{-1}.$$

The matrix $(\mathbf{H}^\top \mathbf{H})^{-1}$ is commonly referred to as the GDOP matrix. Hence, the quality of the estimation depends on the receiver-to-SOP geometry and the pseudo-range observation noise variance. The GDOP factor is defined as $\text{GDOP} \triangleq \sqrt{\text{tr}[(\mathbf{H}^\top \mathbf{H})^{-1}]}$. The GDOP provides a simple scalar characterization of the receiver-to-SOP geometry—the lower the GDOP, the more favorable the geometry [29]. Therefore, the receiver placement problem can be cast as the GDOP minimization problem

$$\underset{\phi_{N+1}}{\text{minimize}} \quad \sqrt{\text{tr}[(\mathbf{H}^\top(\phi_{N+1})\mathbf{H}(\phi_{N+1}))^{-1}]}, \quad (3)$$

where ϕ_{N+1} is the angle of the unit LOS vector from the SOP to the additional $(N+1)$ st receiver location.

The GDOP is approximately minimized when $\det(\mathbf{H}^\top \mathbf{H})$ is maximized, since the adjoint of $\mathbf{H}^\top \mathbf{H}$ varies less with the geometry of the receiver placement [29]. Therefore, an alternative optimization problem to (3) is

$$\underset{\phi_{N+1}}{\text{maximize}} \quad \det[\mathbf{H}^\top(\phi_{N+1})\mathbf{H}(\phi_{N+1})]. \quad (4)$$

It can be shown that $\det(\mathbf{H}^\top \mathbf{H})$ is related to the area of the polytope inscribed in the unit circle, whose vertices are defined by the SOP-to-receiver unit LOS vector endpoints [21]. Hence, the optimization problem can be reformulated as a polytope area maximization problem. In a planar scenario composed of three receivers, the relationship is exact, i.e., maximizing $\det(\mathbf{H}^\top \mathbf{H})$ simultaneously

maximizes the area of the triangle whose vertices are defined by the unit LOS vectors. This is due to the fact that \mathbf{H} is now a square, invertible matrix and the area is $A = \frac{1}{2} \sqrt{\det(\mathbf{H}^\top \mathbf{H})} = \frac{1}{2} \det(\mathbf{H})$. For more than three receivers, the relationship is exact for regular polygons, but approximate for non-regular polygons. Specifically, a polygon inscribed in the unit circle that simultaneously maximizes the determinant and maximizes the area is a regular polygon [30]. For non-regular polygons, the relationship is “almost exact” and the discrepancy is minimal. To see this, $N+1$ receivers were placed randomly around an SOP, where the i th receiver position was chosen such that $\phi_i \sim U(0, 2\pi)$, for $i = 2, \dots, N+1$, and $\phi_1 = 0$ for a total of 10^5 random configurations. For each configuration, the corresponding GDOP and area were calculated, which are plotted in Fig. 1(a)–(d) for $N = 2, \dots, 5$, respectively. Subsequently, for each of the configurations, the first N receivers' positions were fixed and the $(N+1)$ st receiver was placed so to optimize the GDOP then to optimize the area. The resulting optimal GDOP versus optimal area are plotted in Fig. 1(e)–(h) for $N = 2, \dots, 5$, respectively.

The following can be concluded from these plots. First, placing the $(N+1)$ st receiver to optimize the area simultaneously optimizes the GDOP only for $N = 2$. Second, for $N > 2$, placing the $(N+1)$ st receiver to optimize the area approximately optimizes the GDOP. Third, the voids in the “point cloud” in the optimal area versus optimal GDOP plot [Fig. 1(e)–(h)] compared to the area versus GDOP plot [1(a)–(d)] is due to optimizing the placement of the $(N+1)$ st receiver, which effectively increases the area (decreases the GDOP), pushing the “point cloud” towards the right (bottom). Fourth, when $N+1$ receivers are arranged into a regular polygon configuration, the theoretical minimum GDOP, given by $\text{GDOP}_{\min} = \sqrt{5/(N+1)}$ is achieved (dotted red line in Fig. 1) [22] and the area simultaneously achieves its maximum value.

Motivated by these results, an alternative optimization problem to (3) and (4) is proposed, which aims to maximize the area A of the polygon over the angle of the unit LOS vector of interest, namely

$$\underset{\phi_{N+1}}{\text{maximize}} \quad A(\phi_{N+1}) = A_N + \Delta A(\phi_{N+1}), \quad (5)$$

where A_N is the total area for N receivers, which can be derived from the the sum of triangles area as

$$A_N = \sum_{i=1}^N \frac{1}{2} \sin(\theta_i), \quad (6)$$

where $\theta_i \triangleq \phi_{i+1} - \phi_i$ for $i = 1 \dots N-1$, and $\theta_N \triangleq 2\pi - \phi_N$; and $\Delta A(\phi_{N+1})$ is the change in area resulting from placing the $(N+1)$ st receiver at ϕ_{N+1} , where $\phi_i \leq \phi_{N+1} \leq \phi_{i+1} < 2\pi$. The change in area $\Delta A(\phi_{N+1})$ is given by

$$\Delta A(\phi_{N+1}) = \frac{1}{2} [\sin(\phi_{N+1} - \phi_i) + \sin(\theta_i - \phi_{N+1} + \phi_i) - \sin(\theta_i)]. \quad (7)$$

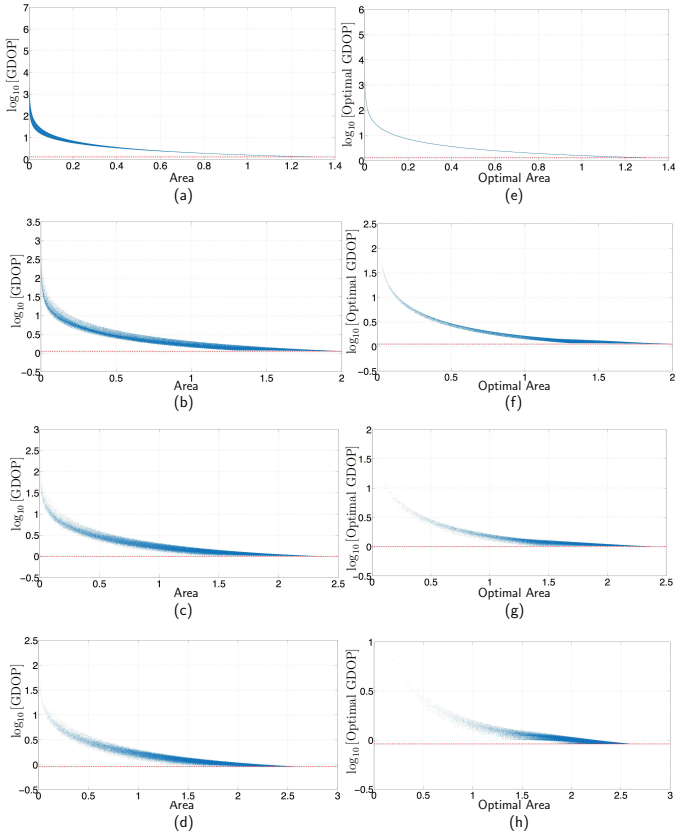


Fig. 1. $N + 1$ receivers were randomly placed around an SOP for a total of 10^5 configurations. Fig. (a)–(d) correspond to $N = 2, \dots, 5$, respectively, and Fig. (e)–(f) correspond to $N = 2, \dots, 5$, respectively. For each configuration, the resulting area and the resulting GDOP were computed and plotted in Fig. (a)–(d). Each point in the point cloud represent the area and corresponding GDOP for a particular configuration. Then, for each previous configuration, the first N receiver locations were fixed and the $(N + 1)^{\text{st}}$ receiver was optimally placed to optimize the GDOP and then to optimize the area. Each point in the point cloud plotted in Fig. (e)–(h) represent the optimal area versus optimal GDOP for a particular configuration.

A depiction of $A(\phi_{N+1})$ is illustrated in Fig. 2.

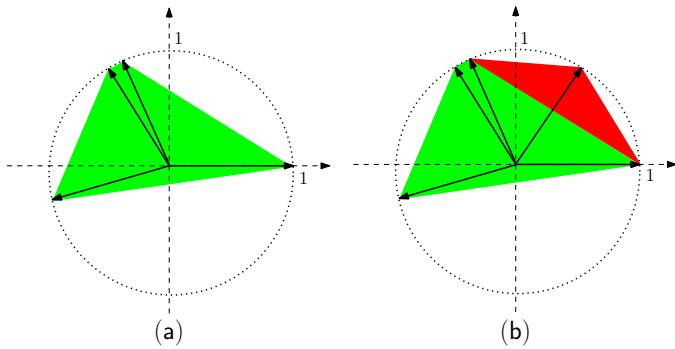


Fig. 2. (a) Polygon inscribed in the unit circle formed by the end-points of the unit LOS vectors from the SOP to four randomly-deployed receivers depicted in Fig. 3(a). The area A_N is highlighted in green. (b) Resulting polygon due to introducing an additional fifth receiver depicted in Fig. 3(a). The change in area $\Delta A(\phi_{N+1})$ due to introducing the $(N + 1)^{\text{st}}$ receiver is highlighted in red.

It will be discussed in the following subsection that unlike

(3) and (4), which are neither convex nor concave, necessitating a general-purpose numerical nonlinear optimization solver, the optimization problem (5) is piecewise-concave with a simple analytical solution.

B. Convexity Analysis

The term $\mathbf{H}^T \mathbf{H}$ in the optimization problems (3) and (4) can be readily shown to be

$$\mathbf{H}^T \mathbf{H} = \begin{bmatrix} \sum_{i=1}^{N+1} \cos^2 \phi_i & \sum_{i=1}^{N+1} \cos \phi_i \sin \phi_i & \sum_{i=1}^{N+1} \cos \phi_i \\ \sum_{i=1}^{N+1} \sin \phi_i \cos \phi_i & \sum_{i=1}^{N+1} \sin^2 \phi_i & \sum_{i=1}^{N+1} \sin \phi_i \\ \sum_{i=1}^{N+1} \cos \phi_i & \sum_{i=1}^{N+1} \sin \phi_i & N + 1 \end{bmatrix}.$$

It is obvious that the optimization functions in (3) and (4) are neither convex nor concave. However, while the optimization function (5) is neither convex nor concave, it is piecewise-concave. A depiction of these functions is illustrated in Fig. 3.

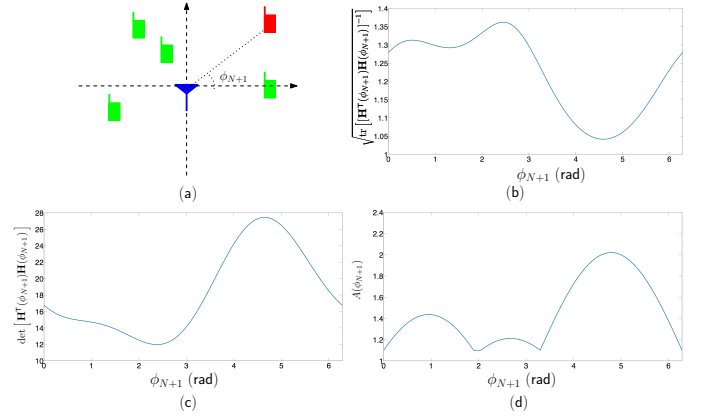


Fig. 3. (a) Four randomly placed receivers (green) with respective angles $\phi_i \in \{0, 1.892, 2.043, 3.295\}$ rad estimating the state vector of an unknown SOP (blue). The optimal receiver placement problem is to place an additional receiver (red) at an angle ϕ_{N+1} that will minimize the GDOP (3), maximize the determinant of the GDOP matrix (4), or maximize the area of the polygon (5). (b)–(d) The corresponding GDOP, determinant, and area optimization functions due to different placements of the additional receiver.

C. Optimal Solution to Area Maximization

The special property of piecewise-concavity of the area maximization problem (5) allows for a simple analytical solution for the receiver placement problem. This is summarized in the following theorem.

Theorem 1. *The optimal placement with respect to the area maximization criterion (5) of a receiver to an environment comprising N arbitrarily placed receivers and one SOP is anywhere on a LOS vector from the SOP at an angle $\phi_{N+1}^* = \frac{1}{2} \max_i \theta_i$, for $i = 1, \dots, N - 1$, where $\theta_i \triangleq \phi_{i+1} - \phi_i$ and $\theta_N \triangleq 2\pi - \phi_N$.*

Proof. First, it will be shown that in a particular $\theta_i \in [0, 2\pi)$, the angle that maximizes the change in area is at $\phi_{N+1}^{*(i)}$, where $\phi_{N+1}^{*(i)} \triangleq \phi_i + \alpha_i^*$ and $\alpha_i^* = \frac{1}{2}\theta_i$, where α_i is defined as the angle sweeping θ_i , i.e., $\alpha_i \triangleq \phi_{N+1} - \phi_i$ for $0 \leq \alpha_i \leq \theta_i$.

Parameterizing $\Delta A(\phi_{N+1})$ by α_i in (7) yields

$$\Delta A(\alpha_i) = \frac{1}{2} [\sin(\alpha_i) + \sin(\theta_i - \alpha_i) - \sin(\theta_i)], \quad (8)$$

and applying the first-order necessary condition for optimality yields

$$\begin{aligned} \frac{d\Delta A(\alpha_i)}{d\alpha_i} &= \frac{1}{2} \cos(\alpha_i) - \frac{1}{2} \cos(\theta_i - \alpha_i) \equiv 0 \\ \Rightarrow \alpha_i^* &= \frac{1}{2} \theta_i + \pi k. \end{aligned}$$

Substituting α^* into the definition of $0 \leq \alpha_i \leq \theta_i$ yields $-\frac{1}{2}\theta_i \leq \pi k \leq \frac{1}{2}\theta_i$. Since the angle between any two known receivers is $0 \leq \theta_i < 2\pi$, k is bounded by $-\pi < \pi k < \pi$. The only value of k that satisfies this inequality is $k = 0$. Therefore, $\alpha_i^* = \frac{1}{2}\theta_i$ is the only critical angle in θ_i .

Furthermore, since $0 \leq \theta_i < 2\pi$, the critical angle is $0 \leq \alpha_i^* < \pi$. The second order necessary condition for optimality, evaluated at this critical angle is

$$\begin{aligned} \frac{d^2 \Delta A_i}{d\alpha_i^2} &= -\frac{1}{2} \sin(\alpha_i) - \frac{1}{2} \sin(\theta_i - \alpha_i) \\ &= -\frac{1}{2} \sin(\alpha_i^*) - \frac{1}{2} \sin(2\alpha_i^* - \alpha_i^*) \\ &= -\sin(\alpha_i^*). \end{aligned} \quad (9)$$

Since (9) is always negative, the change in area in (7) is concave over $\phi_i + \theta_i$, and α^* is the global maximizer. The above analysis holds $\forall \theta_i$, and the change in area over $[0, 2\pi)$ is piecewise-concave with N concave regions, where each region corresponds to $\{\theta_i\}_{i=1}^N$.

Next, it will be shown that the largest change in area $\Delta A(\phi_{N+1})$ is achieved when the largest region θ_i is chosen, i.e., the receiver is positioned at $\phi_{N+1}^* = \phi_{i_{\max}} + \alpha_{i_{\max}}^*$, where $\phi_{i_{\max}} = \phi_{i_{\max+1}} - \theta_{i_{\max}}$, $\theta_{i_{\max}} \triangleq \max_i \{\theta_i\}$, $\alpha_{i_{\max}}^* = \frac{1}{2}\theta_{i_{\max}}$, where $i = 1, \dots, N$.

Substituting for $\alpha_i^* = \frac{1}{2}\theta_i$ into (8) yields

$$\Delta A(\alpha_i^*) = \sin\left(\frac{1}{2}\theta_i\right) - \frac{1}{2} \sin(\theta_i).$$

Taking the derivative with respect to θ_i yields

$$\frac{d\Delta A(\alpha_i)}{d\theta_i} = \frac{1}{2} \cos\left(\frac{1}{2}\theta_i\right) - \frac{1}{2} \cos(\theta_i). \quad (10)$$

Equation (10) is non-negative from $[0, \frac{4\pi}{3}]$, i.e., increasing the region $\theta_i \in [0, \frac{4\pi}{3}]$ increases the resulting area. Hence,

choosing $\theta_{i_{\max}}$ in this range guarantees the largest change in area. In $(\frac{4\pi}{3}, 2\pi)$, (10) is negative, therefore the change in area begins to decrease as θ_i sweeps $(\frac{4\pi}{3}, 2\pi)$. To verify that choosing $\theta_{i_{\max}}$ is the optimal choice, it is shown that $\Delta A(\theta_i) < \Delta A(\theta_{i_{\max}})$, when $\theta_i \in [0, 2\pi - \Gamma]$, where $\Gamma = \theta_{i_{\max}} = \frac{4\pi}{3} + \varepsilon$, $0 < \varepsilon < \frac{2\pi}{3}$. Hence,

$$\begin{aligned} \Delta A(\theta_{i_{\max}}) &> \Delta A(\theta_i) \\ \sin\left(\frac{1}{2}\Gamma\right) - \frac{1}{2} \sin(\Gamma) &> \sin\left[\frac{1}{2}(2\pi - \Gamma)\right] - \frac{1}{2} \sin(2\pi - \Gamma) \\ &= -\frac{1}{2} \sin(\Gamma) > \frac{1}{2} \sin(\Gamma). \end{aligned}$$

Since $\sin(\Gamma) < 0$, $\forall \varepsilon \in (0, \frac{2\pi}{3})$, the above inequality holds and $\Delta A(\theta_{i_{\max}}) > \Delta A(\theta_i)$. \square

IV. OPTIMAL ESTIMATION PERFORMANCE ANALYSIS

This section analyzes the optimal SOP estimation performance as a function of the number of mobile receivers in the environment and time. The optimal performance prescribes the minimum number of receivers needed to achieve a certain mapping accuracy within a desired time horizon.

A. Problem Formulation

The following problem is considered. Given a set of N mobile receivers with knowledge about their own states making pseudorange observations on an unknown terrestrial SOP. Assuming that these observations are fused through a dynamic centralized estimator, specifically an extended Kalman filter (EKF), to estimate the state vector of the SOP, what is the optimal estimation performance as a function of N and time?

In contrast to Section III, which analyzed the optimal placement of the $(N + 1)^{\text{st}}$ receiver, given a set of N randomly-distributed receivers, the optimal performance for the problem here is a function of the placement of all the receivers, simultaneously. Specifically, the optimization is over all the receiver angles $\{\phi_i\}_{i=1}^N$. Assuming the receivers' observation noise to be independent and identically-distributed, the optimal achieved performance is essentially determined by the geometric placement of the receivers. The lowest GDOP is achieved when the unit LOS vectors pointing from the SOP to the receivers reside at the vertices of a regular polygon [22]. Therefore, an environment consisting of N optimally-placed receivers, each drawing pseudorange observations on the same SOP modifies the Jacobian matrix in (2) to take the form

$$\mathbf{H}^* = \begin{bmatrix} -\cos \frac{2\pi 0}{N} & -\sin \frac{2\pi 0}{N} & -1 & 0 \\ -\cos \frac{2\pi}{N} & -\sin \frac{2\pi}{N} & -1 & 0 \\ \vdots & \vdots & \vdots & \vdots \\ -\cos \frac{2\pi(N-1)}{N} & -\sin \frac{2\pi(N-1)}{N} & -1 & 0 \end{bmatrix}. \quad (11)$$

Next, consider the estimation error covariance update equation of the EKF in the information form

$$\mathbf{P}^{-1}(k+1|k+1) = \mathbf{P}^{-1}(k+1|k) + \frac{1}{\sigma^2} \mathbf{H}^\top(k+1) \mathbf{H}(k+1),$$

where $\mathbf{P}(k+1|k+1)$ is the estimation error covariance and $\mathbf{P}(k+1|k)$ is the prediction error covariance. The information associated with the latest observation (at time $k+1$) is $\Upsilon(k+1) = \frac{1}{\sigma^2} \mathbf{H}^\top(k+1) \mathbf{H}(k+1)$. If the receivers are placed optimally, plugging (11) into $\Upsilon(k+1)$ yields

$$\Upsilon(k+1) = \text{diag} \left[\frac{N}{2}, \frac{N}{2}, N, 0 \right],$$

which is independent of the SOP's state vector estimate and receiver trajectories. Noting that the SOP's dynamics are linear, it is obvious that the prediction error covariance $\mathbf{P}(k+1|k)$ is then independent of the SOP's state vector estimate. Therefore, if the receivers maintain their optimal distribution around the latest SOP's position estimate $\hat{\mathbf{r}}_s$ at the time instants when new observations are taken, the estimation error covariance can be propagated off-line, without knowledge of the SOP's state vector estimates nor the receivers' trajectories. The resulting estimation error covariance time history is the optimal estimation error performance as a function of time and number of receivers N .

B. Simulation Results

This subsection presents simulation results demonstrating the optimal estimation performance as a function of time and N . Moreover, the estimation error obtained from random receiver trajectories is compared with the optimal estimation performance.

The optimal posterior estimation error covariance was generated using the following settings: $T = 0.2\text{s}$, $\sigma^2 = 100\text{m}^2$, $\mathbf{P}_s(0|-1) = (10^3) \cdot \text{diag}[1, 1, 3, 0.3]$, and $\mathbf{Q}_s = \text{diag}[\mathbf{0}_{2 \times 2}, c^2 \mathbf{Q}_{\text{clk},s}]$, where

$$\mathbf{Q}_{\text{clk},s} = \begin{bmatrix} \frac{h_0}{2}T + \frac{2}{3}\pi^2 h_{-2}T^3 & \pi^2 h_{-2}T^2 \\ \pi^2 h_{-2}T^2 & 2\pi^2 h_{-2}T \end{bmatrix},$$

with $h_0 = 8.0 \times 10^{-20}$, and $h_{-2} = 4.0 \times 10^{-23}$ as the frequency random walk and white frequency coefficients, respectively [9].

Fig. 4 illustrates the logarithm of the determinant of the posterior estimation error covariance, $\log\{\det[\mathbf{P}^*(k+1|k+1)]\}$, which is proportional to the volume of the estimation uncertainty ellipsoid [17], as a function of time and N . This plot provides the minimum achievable uncertainty of the states of an unknown SOP as a function of time and N . This plot can be utilized to determine the minimum number of receivers that must be deployed in an environment to achieve a desired estimation uncertainty within a specified time horizon.

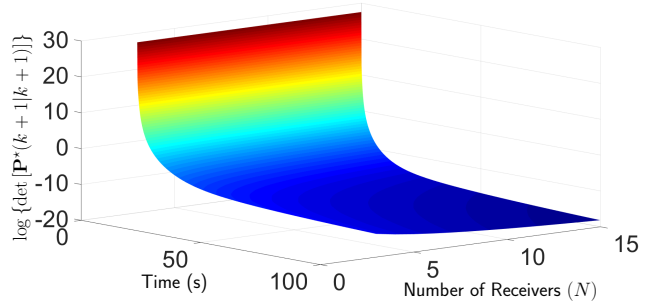


Fig. 4. The logarithm of the determinant of the optimal posterior estimation error covariance $\log\{\det[\mathbf{P}^*(k+1|k+1)]\}$ expressed as a function of time and $N \in \{3, 4, \dots, 15\}$.

To compare the optimal estimation performance versus receiver trajectories that do not maintain the optimal receiver placement around the SOP's position estimate, four receivers were randomly placed around the SOP. The SOP's initial estimate was drawn according to $\hat{\mathbf{x}}_s(0|-1) \sim \mathcal{N}[\mathbf{x}_s(0), \mathbf{P}_s(0|-1)]$, with $\mathbf{x}_s(0) = [0, 0, 1, 0.1]^\top$. The initial state vector of the i^{th} receiver was set to $\mathbf{x}_{r_i}(0) = [\mathbf{r}_{r_i}(0), \dot{\mathbf{r}}_{r_i}(0), c\delta t_{r_i}(0), c\dot{\delta}t_{r_i}(0)]^\top$, where $\dot{\mathbf{r}}_{r_i}(0) = [0, 0]^\top$, $c\delta t_{r_i}(0) = 10$, and $c\dot{\delta}t_{r_i}(0) = 1$. The receivers' initial positions $\mathbf{r}_{r_i}(0)$ are specified in Table I. The receivers' initial positions were varied across three simulation runs, by varying an offset $\{\mathbf{b}_j\}_{j=1}^3$. Subsequently, the receivers moved according to a velocity random walk motion with an acceleration process noise power spectral density $\tilde{q}_x = \tilde{q}_y = 0.1(\text{m/s}^2)^2$ [16]. The receivers' trajectories across the three simulation runs (corresponding to $j = 1, 2, 3$) were the same in order to analyze the effect of the initial GDOP. The time history of the resulting $\log\{\det[\mathbf{P}^j(k+1|k+1)]\}$ corresponding to $j = 1, 2, 3$ versus the optimal $\log\{\det[\mathbf{P}^*(k+1|k+1)]\}$ are plotted in Fig. 5.

TABLE I
SIMULATION SETTINGS FOR THE RECEIVERS' INITIAL POSITION

Parameter	Value
$\mathbf{r}_{r_1}^j(0)$	$[-150.8, 169.3]^\top + \mathbf{b}_j$
$\mathbf{r}_{r_2}^j(0)$	$[24.6, -13.7]^\top + \mathbf{b}_j$
$\mathbf{r}_{r_3}^j(0)$	$[-25.6, -45.5]^\top + \mathbf{b}_j$
$\mathbf{r}_{r_4}^j(0)$	$[105.7, -29.6]^\top + \mathbf{b}_j$
$\mathbf{b}_1, \mathbf{b}_2, \mathbf{b}_3$	$[0, 0]^\top, [125, 0]^\top, [200, 0]^\top$

V. CONCLUSIONS

This paper studied the problem of optimal receiver placement in a COpNav environment comprising N pre-deployed receivers with a random initial distribution. Three optimization problems were formulated and compared: minimizing the GDOP, maximizing the determinant of the GDOP matrix, and maximizing the area of

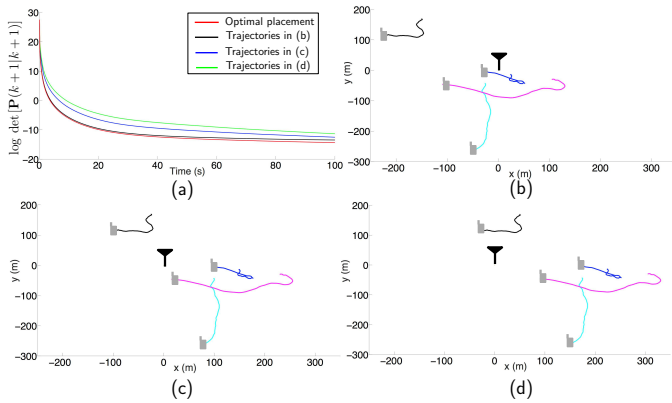


Fig. 5. The logarithm of the determinant of the optimal posterior estimation error covariance $\log \{\det [\mathbf{P}^*(k+1|k+1)]\}$ versus the posterior estimation error covariance due to three simulation runs with the receiver trajectories in (b)–(d). The receivers’ trajectories in (b)–(d) are the same. The receivers’ initial positions in (b)–(d) were varied according to an offset \mathbf{b}_j to yield different initial GDOP quality: (b) low GDOP with \mathbf{b}_1 , (c) medium GDOP with \mathbf{b}_2 , and (d) high GDOP with \mathbf{b}_3 .

a polygon inscribed in the unit circle whose vertices are the endpoints of unit LOS vectors from the SOP to the receivers. It was shown that the area maximization problem is piecewise-concave with a simple analytical solution. Moreover, this paper derived the optimal estimation performance as a function of time and number of receivers in the environment.

References

- [1] J. Raquet and R. Martin, “Non-GNSS radio frequency navigation,” in *Proceedings of IEEE International Conference on Acoustics, Speech and Signal Processing*, March 2008, pp. 5308–5311.
- [2] K. Pesyna, Z. Kassas, J. Bhatti, and T. Humphreys, “Tightly-coupled opportunistic navigation for deep urban and indoor positioning,” in *Proceedings of ION GNSS Conference*, September 2011, pp. 3605–3617.
- [3] V. Moghtadaiee and A. Dempster, “Indoor location fingerprinting using FM radio signals,” *IEEE Transactions on Broadcasting*, vol. 60, no. 2, pp. 336–346, June 2014.
- [4] C. Yang, T. Nguyen, and E. Blasch, “Mobile positioning via fusion of mixed signals of opportunity,” *IEEE Aerospace and Electronic Systems Magazine*, vol. 29, no. 4, pp. 34–46, April 2014.
- [5] P. Thevenon, S. Damien, O. Julien, C. Macabiau, M. Bousquet, L. Ries, and S. Corazza, “Positioning using mobile TV based on the DVB-SH standard,” *NAVIGATION, Journal of the Institute of Navigation*, vol. 58, no. 2, pp. 71–90, 2011.
- [6] K. Pesyna, Z. Kassas, and T. Humphreys, “Constructing a continuous phase time history from TDMA signals for opportunistic navigation,” in *Proceedings of IEEE/ION Position Location and Navigation Symposium*, April 2012, pp. 1209–1220.
- [7] I. Bisio, M. Cerruti, F. Lavagetto, M. Marchese, M. Pastorino, A. Randazzo, and A. Sciarone, “A trainingless WiFi fingerprint positioning approach over mobile devices,” *IEEE Antennas and Wireless Propagation Letters*, vol. 13, pp. 832–835, 2014.
- [8] Z. Kassas and T. Humphreys, “The price of anarchy in active signal landscape map building,” in *Proceedings of IEEE Global Conference on Signal and Information Processing*, December 2013, pp. 165–168.
- [9] Z. Kassas, V. Ghadiok, and T. Humphreys, “Adaptive estimation of signals of opportunity,” in *Proceedings of ION GNSS Conference*, September 2014, pp. 1679–1689.
- [10] Z. Kassas and T. Humphreys, “Observability analysis of opportunistic navigation with pseudorange measurements,” in *Proceedings of AIAA Guidance, Navigation, and Control Conference*, vol. 1, August 2012, pp. 1209–1220.
- [11] —, “Observability and estimability of collaborative opportunistic navigation with pseudorange measurements,” in *Proceedings of ION GNSS Conference*, September 2012, pp. 621–630.
- [12] —, “Observability analysis of collaborative opportunistic navigation with pseudorange measurements,” *IEEE Transactions on Intelligent Transportation Systems*, vol. 15, no. 1, pp. 260–273, February 2014.
- [13] S. Wu, J. Kaba, S. Mau, , and T. Zhao, “Teamwork in GPS-denied environments: Fusion of multi-sensor networks,” *GPS World*, pp. 40–47, Oct. 2009.
- [14] C. Yang and A. Soloviev, “Covariance analysis of spatial and temporal effects of collaborative navigation,” *NAVIGATION, Journal of the Institute of Navigation*, vol. 61, no. 3, pp. 213–225, 2014.
- [15] Z. Kassas, “Collaborative opportunistic navigation,” *IEEE Aerospace and Electronic Systems Magazine*, vol. 28, no. 6, pp. 38–41, 2013.
- [16] —, “Analysis and synthesis of collaborative opportunistic navigation systems,” Ph.D. dissertation, The University of Texas at Austin, USA, 2014.
- [17] Z. Kassas and T. Humphreys, “Motion planning for optimal information gathering in opportunistic navigation systems,” in *Proceedings of AIAA Guidance, Navigation, and Control Conference*, August 2013, 551–4565.
- [18] Z. Kassas, J. Bhatti, and T. Humphreys, “Receding horizon trajectory optimization for simultaneous signal landscape mapping and receiver localization,” in *Proceedings of ION GNSS Conference*, September 2013, pp. 1962–1969.
- [19] Z. Kassas, A. Arapostathis, and T. Humphreys, “Greedy motion planning for simultaneous signal landscape mapping and receiver localization,” *IEEE Journal of Selected Topics in Signal Processing*, vol. 9, no. 2, pp. 247–258, March 2015.
- [20] Z. Kassas and T. Humphreys, “Receding horizon trajectory optimization in opportunistic navigation environments,” *IEEE Transactions on Aerospace and Electronic Systems*, vol. 51, no. 2, pp. 866–877, April 2015.
- [21] P. Massat and K. Rudnick, “Geometric formulas for dilution of precision calculations,” *NAVIGATION, Journal of the Institute of Navigation*, vol. 37, no. 4, pp. 379–391, 1990.
- [22] N. Levanon, “Lowest GDOP in 2-D scenarios,” *IEE Proceedings Radar, Sonar and Navigation*, vol. 147, no. 3, pp. 149–155, 2000.
- [23] I. Sharp, K. Yu, and Y. Guo, “GDOP analysis for positioning system design,” *IEEE Transactions on Vehicular Technology*, vol. 58, no. 7, pp. 3371–3382, 2009.
- [24] N. Blanco-Delgado and F. Nunes, “Satellite selection method for multi-constellation GNSS using convex geometry,” *IEEE Transactions on Vehicular Technology*, vol. 59, no. 9, pp. 4289–4297, November 2010.
- [25] H. Zhang, “Two-dimensional optimal sensor placement,” *IEEE Transactions on Systems, Man and Cybernetics*, vol. 25, no. 5, pp. 781–792, May 1995.
- [26] D. Jourdan and N. Roy, “Optimal sensor placement for agent localization,” in *Proceedings of IEEE/ION Position, Location, And Navigation Symposium*, April 2006, pp. 128–139.
- [27] J. Isaacs, D. Klein, and J. Hespanha, “Optimal sensor placement for time difference of arrival localization,” in *Proceedings of IEEE Conference on Decision and Control*, December 2009, pp. 7878–7884.
- [28] C. Yang, L. Kaplan, E. Blasch, and M. Bakich, “Optimal placement of heterogeneous sensors for targets with Gaussian priors,” *IEEE Transactions on Aerospace and Electronic Systems*, vol. 49, no. 3, pp. 1637–1653, July 2013.
- [29] J. Spilker, Jr., *Global Positioning System: Theory and Applications*. Washington, D.C.: American Institute of Aeronautics and Astronautics, 1996, ch. 5: Satellite Constellation and Geometric Dilution of Precision, pp. 177–208.
- [30] N. Blanco-Delgado, F. Nunes, and G. Seco-Granados, “Relation between GDOP and the geometry of the satellite constellation,” in *International Conference on Localization and GNSS*, Jun. 2011, pp. 175–180.